

ELASTIC WAVEFIELD INVERSION

A DISSERTATION
SUBMITTED TO THE DEPARTMENT OF GEOPHYSICS
AND THE COMMITTEE ON GRADUATE STUDIES
OF STANFORD UNIVERSITY
IN PARTIAL FULFILLMENT OF THE REQUIREMENTS
FOR THE DEGREE OF
DOCTOR OF PHILOSOPHY


By
Peter Mora
July, 1987

© Copyright 1987
by
Peter Mora

printed as Stanford Exploration Project No. 52
by permission of the author

Copying for all internal purposes of the sponsors
of the Stanford Exploration Project is permitted

I certify that I have read this thesis and that in my opinion it is fully adequate, in scope and in quality, as a dissertation for the degree of Doctor of Philosophy.



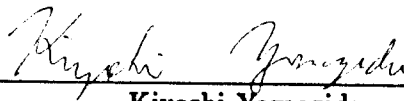
Jon F. Claerbout
(Principal Advisor)

I certify that I have read this thesis and that in my opinion it is fully adequate, in scope and in quality, as a dissertation for the degree of Doctor of Philosophy.



Francis Muir

I certify that I have read this thesis and that in my opinion it is fully adequate, in scope and in quality, as a dissertation for the degree of Doctor of Philosophy.



Kiyoshi Yomogida

Approved for the University Committee on Graduate Studies:

Dean of Graduate Studies & Research

Elastic wavefield inversion

*Peter Mora, Ph.D.
Stanford University, 1987*

ABSTRACT

The goal of seismology is to obtain Earth properties from seismic data. I derive formulas based on nonlinear least squares iterations to find the elastic properties of the Earth corresponding to the synthetic wavefield that best matches the seismic observations. Primary P- and S-wave reflections, mode converted waves and Rayleigh waves are all theoretically useful in the inversions. Beginning with a starting guess, the Earth properties are iteratively updated using a preconditioned conjugate-gradient algorithm. The gradient direction is cast in terms of two wave propagations so Frechet matrices are not necessary and the calculations are easily implemented on fine grain parallel computers.

Although the derivation is in three dimensions and commences from the anisotropic elastic wave equation, I have chosen to concentrate on the special case of an isotropic Earth and solve for the compressional and shear wavespeeds. This case is important because the wavespeeds are the properties that have the largest influence on seismic waves. The sudden (high-wavenumber) variations in the wavespeeds at layer boundaries determine the amplitudes of reflected waves while the gross (low-wavenumber) variations in the layers determine the traveltimes of reflected and transmitted waves.

The method is tested by inverting 2D synthetic reflection seismograms (shot profiles), 2D synthetic transmission seismograms (VSP's) and real reflection seismograms (a shot profile). The wave propagations in the tests are done using elastic finite differences to allow for Earth models of realistic complexity. The synthetic data results indicate that low-wavenumber components in wavespeed converge slowly when only reflection data were inverted. This was not expected considering that traveltime curves of reflections should rapidly resolve the low wavenumbers. However, by analyzing an acoustic equivalent of the algorithm in detail, I have identified reflection-tomography-like terms and migration-like terms in the inversion formulas. I prove that the low wavenumbers are resolved by the tomography-like terms and suggest how to get an even rate of convergence of the high and low wavenumbers. I conclude that my iterative elastic inversion formulas obtain all

wavenumbers of the compressional and shear wavespeeds that are resolvable separately by migration and tomography.

I propose that the main topics for future research in seismic wavefield inversion are: how to eliminate the need for an initial model, how to model seismic waves more accurately, how to resolve additional Earth properties, and how to allow for non-Gaussian distributed noise and Earth properties.

Preface

Finally, both the theory and computer power make it feasible to throw away ad hoc methods and partial solutions. Seismic observations can be fed into computers and Earth models will pop out. This goal is on the verge of being realized! Read on.

Acknowledgements

I'd like to express my gratitude to Jon Claerbout for creating the perfect research environment. He nurtures the concept of academic freedom. I have never met anyone with higher scientific morals and he has my utmost admiration and respect.

Next, I would like to thank Albert Tarantola who has been the source of many ideas and who has had a great impact on my Ph.D. research. Without his encouragement and support I doubt any of this research would have come to fruition. His energy level and idealistic approaches, undaunted by excessive pragmatism, have been a constant source of inspiration.

I also want to acknowledge the help of my many fellow students at Stanford. When I arrived at Stanford, the older students acted like patrons, patiently teaching and providing guidance. In particular, Jeff Thorson helped me build a firm foundation for seismic research. Younger students and peers, especially Kamal Al-Yahya, John Toldi, Dan Rothman and Jos Van Trier, were a constant source of interesting discussion, useful comments and suggestions, Others who have contributed in various ways are Chuck Sword, Paul Fowler and Clement Kostov.

During a learning and collaborative period with Albert Tarantola in France, I was aided by many people including Alexandre Nercessian, Jean Virieux, Valerie Lebouc, Manuela Mendes, Antonio Pica, Odille Gauthier, Ligor Nikolla, and Luc Ikelle.

Finally, I want to thank the people who are most important in my life, for without them, I would never have persevered. They provided support and love throughout. They are my parents and close friends, especially, Evelyne Meier.

Contents

Abstract	iv
Preface	vi
Acknowledgements	vii
List of figures	xii
1 Dreaming of inversion	1
1.1 The seismologists' dream	1
1.2 Conventional wisdom fails	2
1.3 Inversion to the rescue	4
2 Observations of elastic waves	5
2.1 Is the earth elastic?	5
2.2 Primary reflections and mode conversions	5
2.3 Other elastic phenomena	12
2.4 Conclusions	12
3 Elastic inversion theory	14
3.1 Overview	14
3.2 Philosophy of inversion	15
3.2.1 Elastic waves or acoustic waves?	15
3.2.2 Inversion or conventional processing?	15
3.2.3 Linear or nonlinear?	16
3.3 Probability theory and least squares	18

3.3.1	Probabilistic inversion	18
3.3.2	Nonlinear least squares	19
3.3.3	Preconditioning	22
3.3.4	Conjugate directions	23
3.3.5	Inversion algorithm	24
3.3.6	Computational aspects for nonlinear functions	24
3.4	Inversion achieved by modeling	25
3.4.1	Overview	25
3.4.2	What is the adjoint operation?	26
3.4.3	What is the adjoint operation for the seismic problem?	28
3.4.4	What is the linearized elastic forward problem?	28
3.4.5	What is the elastic adjoint operation?	30
3.4.6	Interpreting the adjoint	32
3.4.7	The gradient direction	34
3.4.8	Model covariances	35
3.4.9	Data covariances	36
3.4.10	Different model parameters	37
3.5	Inversion described by pictures	39
3.5.1	Introduction	39
3.5.2	Transmission data	39
3.5.3	Reflection data	43
4	Results	50
4.1	Overview	50
4.2	Noisy diffractions	51
4.3	Single component data	58
4.4	Reflection seismic data	61
4.5	Transmission seismic data	71
4.6	Field data	79
4.7	Conclusions	84
5	Solution to the low wavenumber problem	85
5.1	Overview	85
5.2	What is the low wavenumber problem?	86

5.2.1	The problem	86
5.2.2	The problem with the problem	86
5.2.3	Resolution of the problem through assumptions	86
5.2.4	Resolution of the problem through inversion in principle	87
5.2.5	Resolution and understanding through analysis	87
5.3	Are the low wavenumbers resolvable?	87
5.3.1	Insights from pictures	87
5.3.2	Non-constant background scattering	88
5.3.3	Non-constant background inversion	94
5.3.4	The resolved wavenumber spectrum	94
5.3.5	The tomographic terms revealed	98
5.3.6	Relationship to iterative inversion	100
5.3.7	Illustration of inversion	103
5.3.8	Inversion = migration + tomography	107
5.4	Conclusions	109
6	Directions of the future	110
6.1	Is the seismic inverse problem solved?	110
6.1.1	What is the seismic inverse problem?	110
6.1.2	Solving for the initial model	111
6.1.3	Accounting for everything	111
6.1.4	Statistics	111
6.1.5	Parallelism, physics and inverse physics	112
7	Conclusions	113
A	Adequacy of finite differences	114
A.1	Introduction and overview	114
A.1.1	Finite difference scheme	114
A.1.2	Questions of adequacy for inversion	114
A.1.3	Answers	115
A.2	Finite differences compared to Haskell-Thompson	115
A.2.1	Differences in the assumptions	115
A.2.2	Comparison of results	116

A.2.3	Comparison of P-P and P-S reflections	118
A.2.4	Comparison of results using a free surface B.C.	118
A.3	Are free surfaces needed for P-P and P-S amplitudes?	122
A.4	Conclusions	124
B	Verification of the elastic adjoint operation	125
B.1	Overview	125
B.1.1	Testing adjoint implementations	125
B.1.2	1D acoustic tutorial	125
B.1.3	1D acoustic results	126
B.1.4	2D elastic results	126
B.2	Tutorial: the 1D, constant velocity acoustic case	126
B.2.1	Mathematical proof of the adjoint	127
B.2.2	Numerical calculation	128
B.2.3	Algorithm	128
B.2.4	Pseudo code	130
B.2.5	Numerical test	131
B.3	2D elastic dot product test	137
B.3.1	Summary	137
B.3.2	Linearized forward problem	137
B.3.3	Numerical result	139
B.4	Conclusions	139
	Bibliography	141

List of Figures

2.1	Two-component field shot gather supplied by C.G.G.	7
2.2	Two-component synthetic shot gather computed by elastic theory.	8
2.3	Velocity model used to generate the synthetic data.	9
2.4	Difference between gathers with and without the deep reflector.	10
2.5	Two-component synthetic shot gather computed by acoustic theory.	11
2.6	Field shot gather with Rayleigh waves.	12
3.1	The “camembert” model used to generate transmission data.	40
3.2	Vertical component residual transmission data.	40
3.3	The transmission-data gradient calculations pictorially.	41
3.4	P and S-wave velocity perturbation for the transmission data inversion.	42
3.5	Layer/halfspace model used to generate reflection data.	44
3.6	Vertical component residual shot gather for layer/halfspace model.	44
3.7	The reflection-data gradient calculations pictorially.	45
3.8	P-wave and S-wave velocity perturbation for the reflection data inversion.	46
4.1	Diffractor model relative to a homogeneous background.	52
4.2	Two-component shot gather for the diffractor model.	53
4.3	One and seven iteration P-wave velocity inversion results of diffraction data.	54
4.4	One and seven iteration S-wave velocity inversion results of diffraction data.	55
4.5	One and seven iteration density inversion results of diffraction data.	56
4.6	Two-component mismatch after inverting the diffraction data.	57
4.7	One and seven iteration P-wave velocity inversion result using the vertical component diffraction data.	58
4.8	One and seven iteration S-wave velocity inversion result using the vertical component diffraction data.	59

4.9	One and seven iteration density inversion result using the vertical component diffraction data.	60
4.10	Horst/reef model relative to a linear background function.	62
4.11	A two-component shot gather for the horst/reef model.	63
4.12	One and ten iteration P-wave velocity inversion result using the horst/reef reflection data compared to the filtered P-wave velocity model.	65
4.13	One and ten iteration S-wave velocity inversion result using the horst/reef reflection data compared to the filtered S-wave velocity model.	66
4.14	One and ten iteration density inversion result using the horst/reef reflection data compared to the filtered density model.	67
4.15	Log through the reef (i.e. property versus depth): true model (bold line), initial model (fine line), one iteration result (dotted line) and ten iteration result (broken line).	68
4.16	Vertical wavenumber spectrum of the P-wave velocity log through the reef after one and ten iterations.	69
4.17	Vertical wavenumber spectrum of the true P-wave velocity log through the reef.	69
4.18	Two-component mismatch after ten iterations for the horst/reef example.	70
4.19	A two-component offset VSP for the horst/reef model.	72
4.20	One and ten iteration P-wave velocity inversion result using the horst/reef transmission data compared to the true P-wave velocity model.	73
4.21	One and ten iteration S-wave velocity inversion result using the horst/reef transmission data compared to the true S-wave velocity model.	74
4.22	One and ten iteration density inversion result using the horst/reef transmission data compared to the true density model.	75
4.23	Log through the reef (i.e. property versus depth): true model (bold line), initial model (fine line), one iteration result (dotted line) and ten iteration result (broken line).	76
4.24	Vertical wavenumber spectrum of the P-wave velocity log through the reef after one and ten iterations.	77
4.25	The normalized sum of the square error as a function of iteration number.	77
4.26	Two-component VSP mismatch after ten iterations for the horst/reef example.	78

4.27	Mismatch for the two-component field shot gather at iteration zero.	80
4.28	Mismatch for the two-component field shot gather at iteration three.	81
4.29	The normalized sum of the square error as a function of iteration number.	82
4.30	Three iteration field data inversion result.	83
5.1	Basic plane wave experiment showing plane waves incident on a velocity anomaly embedded in a layer over a halfspace.	88
5.2	Raypaths corresponding to the four different scattering terms.	93
5.3	The part of the wavenumber spectrum of the squared slowness model that can be resolved using a single plane wave source.	95
5.4	The part of the wavenumber spectrum of the squared slowness that can be resolved using a point source (i.e. a sum of plane waves at all angles).	95
5.5	The part of the wavenumber spectrum of squared slowness that can be resolved from the migration-like and tomographic-like terms in the inversion formulas.	97
5.6	Shot gather from a circular-anomaly/layer-halfspace-background model.	98
5.7	The true model compared to the ten iteration inversion result for the circular-anomaly/layer-halfspace-background data using a single shot gather.	99
5.8	One of five shot gathers generated from a circular-anomaly/homogeneous-background model.	103
5.9	True model compared to the one and fifteen iteration inversion results, from the circular-anomaly/homogeneous-background data, using five shot gathers.	104
5.10	One of five shot gathers generated from a circular-anomaly/layer-halfspace-background model.	105
5.11	True model compared to the one and fifteen iteration inversion results, from the circular-anomaly/layer-halfspace-background data, using five shot gathers.	106
A.1	The velocity model.	116
A.2	The pressure source - vertical receiver shot gather via FD (c.f. Figure A.3).	117
A.3	The pressure source - vertical receiver shot gather via Sherwood (c.f. Figure A.2).	117
A.4	The velocity model.	118
A.5	The pressure source - vertical receiver shot gather via FD (c.f. Figure A.6).	119

A.6	The pressure source - vertical receiver shot gather via Sherwood (c.f. Figure A.5).	119
A.7	The difference between Figures A.5 and Figure A.6 (Figure A.5 - Figure A.6).	120
A.8	The vertical source - vertical receiver shot gather via FD (c.f. Figure A.9) computed using a free surface boundary condition.	121
A.9	The vertical source - vertical receiver shot gather via Sherwood (c.f. Figure A.8) computed using an air-solid surface boundary condition.	121
A.10	The difference between Figures A.8 and Figure A.9 (Figure A.8 - Figure A.9).	122
A.11	The vertical source - vertical receiver shot gather via FD (c.f. Figure A.8) computed using an absorbing surface boundary condition.	123
A.12	The difference between Figures A.11 and Figure A.8 (Figure A.11 - Figure A.8) to see the effect of the free surface on the reflections.	123
B.1	The density perturbation vector $\delta\rho = \mathbf{x}$	132
B.2	The density perturbation vector $\delta\rho_1 = \mathbf{x}_1$	132
B.3	The displacement perturbation vector $\delta\mathbf{u} = \mathbf{y} = \mathbf{A}\mathbf{x}_1$	132
B.4	The displacement perturbation vector $\mathbf{A}\mathbf{x}$	133
B.5	The adjoint vector $\delta\hat{\rho} = \mathbf{A}^T\mathbf{x}$	133
B.6	The background wavefield $u(\mathbf{x}, t)$	133
B.7	The perturbation wavefield $\delta v(\mathbf{x}, t)$	134
B.8	The back-propagated residual wavefield $\psi(\mathbf{x}, t)$	134
B.9	The linearized forward problem $\mathbf{A}\mathbf{x}$	138
B.10	The linearized forward problem $\mathbf{A}\mathbf{x}$ shown in Figure B.9 boosted by a factor of 10^3	139